Coumarin linked thiazole derivatives as potential α-Glucosidase inhibitors to treat Diabetes Mellitus

Rushikesh Ichale
   SVKM's NMIMS, SPP School of Pharmacy & Technology Management

Ashish M. Kanhed
   SVKM's NMIMS, SPP School of Pharmacy & Technology Management

Amisha Vora (✉ amisha.Vora@nmims.edu)
   SVKM's NMIMS, SPP School of Pharmacy & Technology Management

Research Article

Additional Declarations: No competing interests reported.

Abstract

Diabetes is a leading cause of kidney failure, blindness, heart attacks and lower limb amputation. Prevalence of diabetes is rising globally. α-glucosidase is validated target for controlling hyperglycemia because of its role in catalysing hydrolysis of carbohydrates to glucose in GIT. In an attempt to find novel safe and effective α-glucosidase inhibitors, coumarin linked thiazole were identified as potential scaffold on the basis of their interactions with the active site of α-glucosidase studied *in silico*. A series of coumarin linked thiazole derivatives were synthesized and analysed for α-glucosidase inhibitory potential in an *in-vitro* assay. The synthesized molecules showed potent inhibition of α-glucosidase with IC_{50} values ranging from 0.14 to 9.38 μM. The most potent compound 2-((4-bromophenyl) amino)-N-(4-(2-oxo-2H-chromen-3-yl) thiazol-2-yl) acetamide was further docked with α-glucosidase and molecular dynamics studies were carried out for 100ns which suggested the stability of protein and ligand in the protein active site over the simulation period and role of hydrophobic interactions slightly more than the electrostatic/polar interactions in ligand-receptor stability. In summary, our results demonstrate efficacy of coumarin-linked thiazole as potential leads for further optimization and development.

Introduction

Diabetes mellitus (DM) is considered one of the world's leading health emergencies in the 21st century. According to WHO report 2021, currently 537 million people are living with diabetes and the number is projected to rise to 700 million by 2045 [1]. It is considered to be one of the major causes of blindness, kidney failure, cardiovascular diseases, neuropathy and many other complications [2]. Type I diabetes, also known as insulin dependent DM (IDDM) is a chronic condition in which β cells of pancreas are attacked by immune system of the body. This condition is prevalent in children and requires treatment with insulin [3]. Type II DM accounts for 90–95% of all DM patients, is characterised by dysfunction of pancreatic beta cells, decrease in insulin secretion and/or insulin resistance [4]. Among the various treatments available are drugs belonging to the class of sulfonylureas, DPP-IV inhibitors, SGLT2 inhibitors, GLP-1 agonists and α-glucosidase inhibitors.

α-glucosidase is a validated target for antidiabetic activity. It is an enzyme that is found to be present in the brush border of small intestine, functions to bring about breakdown of carbohydrates to glucose for absorption through the small-intestine. This leads to rise in glucose levels post meals [5–7]. Currently only three drugs, acarbose, voglibose and miglitol are available in the market as α-glucosidase inhibitors. These molecules require highly complicated multistep synthesis and also suffer from side-effects like diarrhoea, bloating, flatulence and other gastrointestinal disorders [8]. There is a great need to develop safe and efficacious α-glucosidase inhibitors for the treatment of type II DM.

Heterocyclic ring systems like imidazole [9], thiazole [10], azole [11], pyrazole[12] have been widely explored and shown promising α-glucosidase inhibitory activity [13]. This current research involves hybridisation of coumarin and thiazole rings to synthesise a series of coumarin-linked thiazole derivatives and evaluation of their α-glucosidase enzyme inhibitory activity. Molecular docking and

dynamic studies between the most active molecule and α-glucosidase enzyme are further carried out in order to support enzyme inhibition studies.

Result And Discussion

Designing:

To understand the interaction ability of designed scaffold with α-glucosidase enzyme (PDB code: 3TOP), the intermediate scaffold 3-(2-aminothiazol-4-yl)-2*H*-chromen-2-one (**3**) and its aniline derivative (**5**) were docked with the active site of the enzyme. Intermediate **3** showed promising interactions with the active site. Aminothiazole moiety of scaffold exhibited promising pi-anion interactions with TRP1418, ASP1420, TRP1523 and HIS1584. Further the N-H of same moiety stabilized the ligand receptor complex by forming a strong hydrogen bond with ASP1279. Additional stability to the complex was imparted by hydrogen bonding between coumarin C = O with ARG1510. Further, the coumarin moiety of scaffold under analysis was found to be stabilized within active site of receptor by pi-pi interactions with TRP1355 and PHE1560 along with pi-anion interactions with ASP1526. In addition to similar type of interactions, the aniline moiety of compound **5** with acetyl linker provided further stability by showing hydrophobic interaction with hydrophobic pocket comprised of hydrophobic amino acids GLN1561, ASP1562, THR1589 and GLY1588. The additional stability of compound **5** over intermediate **3** was also observed in the interaction energies, where intermediate **3** showed − 6.37 Kcal/mol and compound **5** with − 6.82 Kcal/mol.

Chemistry

The synthesis of 3-acetyl-2*H*-chromen-2-one (**1**) was performed stirring salicylaldehyde, ethyl acetoacetate, piperidine and methanol at room temperature (RT) for 1 hour [14]. To compound **1**, bromine and glacial acetic acid were added at RT. This mixture was subjected to 4 hours continuous stirring to get 3-(2-bromoacetyl)-2*H*-chromen-2-one (**2**) [15]. Compound **2** was reacted with thiourea in ethanol under reflux for 3 hours to get 3-(2-aminithiazol-4-yl)-2*H*-chromen-2-one (**3**) [16]. Cloroacetylation of compound **3** was carried out with chloroacetyl chloride in presence of base triethylamine and chloroform as a solvent under reflux for 6−7 hours to get 2-chloro-*N*-(4-(2-oxo-2*H*- chromen-3-yl) thiazol-2-yl) acetamide (**4**) [17]. Synthesis of various derivatives (**5−24**) was performed by using 2-chloro-*N*-(4-(2-oxo-2*H*-chromen-3-yl) thiazol-2-yl) acetamide (**4**) as starting material along with triethylamine as base, dimethylformamide as solvent and different amines (aniline & benzylamine) at 70 ˚C for 12−14 hours with continuous stirring [18].

Biological study

In Vitro α-glucosidase Enzyme Inhibitory Activity

The α-glucosidase enzyme inhibitory activity of synthesized compounds was carried out as per the standard protocol [19]. As reported in Table 1, all the synthesized derivatives showed inhibitory activity against α-glucosidase enzyme with an IC_{50} value range from 0.144947 to 9.384327 μM. Out of 19 derivatives 13 derivatives shows higher activity than that of acarbose as the positive control (IC_{50} = 6.319947 μM). Among all the synthesized compounds, compound **18** (IC_{50} = 0.144947 μM) showed the highest inhibitory activity.

Table 1
In vitro α-glucosidase enzyme inhibitory activity of compounds (5–19)

Comp Code	IC_{50} (μm)	Comp Code	IC_{50} (μm)
5	2.79	**13**	2.66
6	1.51	**14**	3.71
7	2.80	**15**	8.41
8	3.94	**16**	0.40
9	4.25	**17**	6.09
10	3.45	**18**	0.14
11	5.06	**19**	2.29
12	6.81		
Acarbose (std)		6.32	

Docking Study

To understand the interaction ability of most active compound (**18**) with α-Glucosidase enzyme (PDB code: 3TOP), molecular docking study was performed using AutoDock tools [20–22]. The benzopyran-2-one ring of **18** exhibited promising edge to face pi-pi interactions with Tyr1251, Trp1355 and Phe1559 along with pi-anion interaction with Asp 1526. The thiazole ring also contributed in stabilizing the receptor ligand complex by pi-pi interaction with Phe1560 and pi-sulfur interaction with Trp1355 and Phe1560. The 4-bromophenyl acetamide moiety of **18** found to be well established in hydrophobic pocket of receptor made of Ile1587, Gly1588, Thr1589 and Trp1369. These interactions explain the promising stability of most active compound **18** with α-Glucosidase enzyme active site (Fig. 2a,2b). To understand the time dependant stability of these interactions, 100 ns molecular dynamics study was carried out with this receptor ligand complex.

Molecular Dynamics

The docked complex of compound **18** and α-Glucosidase enzyme (PDB code: 3TOP) was taken as starting frame for molecular dynamics study for 100 ns, and different statistical parameters like RMSD-P, RMSF-P, RMSD-L (*P* = protein, *L* = ligand), H-bonding, van der Waals/hydrophobic (LJ-SR), electrostatic (Coul-SR) interaction energies between ligand-protein etc. were determined. The protein RMSD (RMSD-P) explains the degree of movement of protein residues while having ligand in the receptor active site and suggests the stability, deviation and conformations of the protein structure over the period of simulation time [23–28]. Here the RMSD-P for this receptor-ligand complex was in the range of 0.15 to 0.27 with the average of 0.22 nm. This explains the stability of α-Glucosidase while having compound **18** in receptor active site (Fig. 3a). The average RMSD of ligand while in the receptor active site was 0.23 nm with the range between 0.1 to 0.3 nm suggest the conformational stability of compound **18** in the receptor active site. Despite of having multiple rotatable bonds, the ligand is stable and not carried away from the active site or no major conformational changes in ligand, while in receptor active site, were observed (Fig. 3b). Both these observations strongly suggests the stability of protein and ligand in the protein active site over the simulation period. The RMSF describes the integrity and residual mobility of the protein structure. Here while having ligand in the active site region, including loop and terminal residues the fluctuation was below 0.53 nm suggesting the stability of the system (Fig. 3c). Total hydrogen bonds between ligand-receptor were measured over the simulation duration. Total 5 hydrogen bonds were observed during simulation period, out of which two were stable over more than 80% of simulation duration, suggesting involvement of hydrogen bonding in receptor-ligand stability (Fig. 3d). The short-range electrostatic (Coul-SR), which explains contribution of polar interactions, and van der Waals (LJ-SR), which explains contribution of hydrophobic interactions, energies between ligand-receptor. The average values of Coul-SR − 89.23 ± 5.4 kJ/mol and LJ-SR − 101.54 ± 3.8 kJ/mol were observed. This explains the role of hydrophobic interactions is slightly more than the electrostatic/polar interactions in ligand-receptor stability.

Conclusion

In the conclusion, various novel coumarin linked thiazole derivatives were designed, synthesized, analysed and evaluated for their α-glucosidase enzyme inhibitory activity for the treatment of Type II diabetes. All the compounds inhibited α-glucosidase enzyme and the most potent compound was found to be 2-((4-bromophenyl) amino)-N-(4-(2-oxo-2H-chromen-3-yl) thiazol-2-yl) acetamide **(18)**, with an IC_{50} value of 0.1449 μM. Molecular dynamic studies of were carried out for docked complex of compound 18 with α-glucosidase for 100ns, which explained the importance of hydrophobic interactions in the stability of ligand receptor complex.

Experimental

Chemistry

All the chemical reactions were monitored by using Merck pre coated silica gel 60 F_{254} thin layer chromatography (TLC) plates. The Fourier transform infrared spectroscopy (FTIR) of synthesized

compounds was performed on spectrum2, Perkin instrument. The spectra were recorded post background correction within range of 4000 to 400 cm^{-1} at the resolution of 4 cm^{-1}. The ^{1}H-NMR, spectra was recorded in dimethyl sulfoxide (DMSO) using Bucker 500 MHz NMR instrument. The mass spectra (MS) were recorded on LC-MS model 4080, shimadzu. Biological activity was assist using ultra violet (UV) spectrophotometer (UV-1800, shimadzu corporation).

3-acetyl-2H-chromen-2-one (1)

Yield: 88%; m.p.: 118-122 ˚C; IR (cm^{-1}): 3030.18, 1721.73, 1676.34, 1353.46, 1202.26,756.62; MS (m/z): 189.10 (M+H) $^+$

3-(2-bromoacetyl)-2H-chromen-2-one (2)

Yield: 93%; m.p.: 164-165 ˚C; IR (cm^{-1}):1721.15, 1554.41, 1178.30, 978.56, 155.56; MS (m/z): 266.90(M+2) $^+$

3-(2-aminothiazol-4-yl)-2H-chromen-2-one (3)

Yield:97%; m.p.: 226-229 ˚C; IR (cm^{-1}): 3166.02, 2776.25, 1719.14, 1626.33,1266.42,752.35; MS (m/z): 245(M+H) $^+$

2-chloro-N-(4-(2-oxo-2H-chromen-3-yl)thiazol-2-yl)acetamide (4)

Yield: 91%; m.p.: 204-207 ˚C; IR (cm^{-1}): 2989.89, 1710.96, 1095.19, 792.51; MS (m/z): 321.05 (M+H) $^+$

N-(4-(2-oxo-2H-chromen-3-yl)thiazol-2-yl)-2-(phenylamino)acetamide (5)

Yield: 89%; m.p.: 206-211 ˚C; IR (cm^{-1}):2922.21, 1715.08, 1602.56, 1551.97, 1443.48, 1379.45, 1179.16, 1095.95, 925.56,752.10; ^{1}H-NMR: δppm: 3.55-3.57 (2H, -CH2-), 4.19 (1H, aniline NH), 11.86 (1H, thiazole NH), 8.61 (1H, thiazole CH), 8.12 (1H, coumarone C4-H), 6.57-8.02 (9H, aromatic CH); MS (m/z): 378.25 (M+H) $^+$

2-((4-chlorophenyl)amino)-N-(4-(2-oxo-2H-chromen-3-yl)thiazol-2-yl)acetamide (6)

Yield: 60%; m.p.: 225-228 ˚C; IR (cm^{-1}): 2922.73,1686.35, 1604.14, 1550.53, 1491.69,1252.78, 1178.31, 1093.62, 1024.62, 755.63; ^{1}H-NMR: δppm: 3.55-3.65 (2H, -CH2-), 4.19 (1H, aniline NH), 12.26 (1H, thiazole NH), 8.58 (1H, thiazole CH), 8.10 (1H, coumarone C4-H), 6.55-8.04 (8H, aromatic CH); MS (m/z): 412.30 (M+H) $^+$

2-((4-fluorophenyl)amino)-N-(4-(2-oxo-2H-chromen-3-yl)thiazol-2-yl)acetamide (7)

Yield: 72%; m.p.: 198-204 ˚C; IR (cm^{-1}): 3297.43, 1683.46, 1604.87, 1552.52, 1508.07, 1440.08, 1378.44, 1213.74, 1096.14, 1025.84, 757.18; ^{1}H-NMR: δppm: 3.54-3.56 (2H, -CH2-), 4.19 (1H, aniline NH), 12.31

(1H, thiazole NH), 8.60 (1H, thiazole CH), 8.00 (1H, coumarone C4-H), 6.59-8.00 (8H, aromatic CH); MS (m/z): 395.95 (M+H) $^+$

2-((3,4-dichlorophenyl)amino)-N-(4-(2-oxo-2H-chromen-3-yl)thiazol-2-yl)acetamide (8)

Yield: 73%; m.p.: 209-214 ˚C; IR (cm^{-1}): 2923.15, 1714.62, 1602.53, 1475.70, 1379.25, 1270.40, 754.55; ^{1}H-NMR: δppm: 4.10-4.18 (2H, -CH2-), 4.36 (1H, aniline NH), 12.63 (1H, thiazole NH), 6.74-8.64 (9H, ring CH); MS (m/z): 446.30 (M)$^+$, 448.10 (M+2) $^+$, 450 (M+4)$^+$

2-((4-methoxyphenyl)amino)-N-(4-(2-oxo-2H-chromen-3-yl)thiazol-2-yl)acetamide (9)

Yield: 61%; m.p.: 212-216 ˚C; IR (cm^{-1}): 3297.91, 2924.29, 1709.82, 1686.01, 1605.10, 1555.96, 1509.95, 1378.74, 1244.78, 1177.82, 1030.78, 755.77; ^{1}H-NMR: δppm: 3.54-3.61 (3H, -OCH3), 3.65-3.72 (2H, -CH2-), 4.18 (1H, aniline NH), 12.22 (1H, thiazole NH), 8.62 (1H, thiazole CH), 8.00 (1H, coumarone C4-H), 6.56-7.85 (8H, aromatic CH); MS (m/z): 408.15 (M+H) $^+$

2-((3-methoxyphenyl)amino)-N-(4-(2-oxo-2H-chromen-3-yl)thiazol-2-yl)acetamide (10)

Yield: 66%; m.p.: 228-232 ˚C; IR (cm^{-1}): 3294.79, 2923.88, 1714.65, 1603.11, 1096.01, 755.16; ^{1}H-NMR: δppm: 3.52-3.64 (3H, -OCH3), 3.64-3.70 (2H, -CH2-), 4.19 (1H, aniline NH), 12.36 (1H, thiazole NH), 6.00-8.68 (10H, aromatic CH); MS (m/z): 408.20 (M+H) $^+$

2-((2-chlorophenyl)amino)-N-(4-(2-oxo-2H-chromen-3-yl)thiazol-2-yl)acetamide (11)

Yield: 69%; m.p.: 198-202˚C; IR (cm^{-1}): 2922.82, 2852.20, 1715.24, 1253.85, 1095.20, 752.24; ^{1}H-NMR: δppm: 4.19-4.32 (2H, -CH2-), 4.36 (1H, aniline NH), 12.85 (1H, thiazole NH), 8.62 (1H, thiazole CH), 8.14 (1H, coumarone C4-H), 7.12-8.06 (8H, aromatic CH); MS (m/z): 412.10 (M+H) $^+$

2-((3,5-dichlorophenyl)amino)-N-(4-(2-oxo-2H-chromen-3-yl)thiazol-2-yl)acetamide (12)

Yield: 76%; m.p.: 205-207 ˚C; IR (cm^{-1}):2993.25, 1714, 1591.12, 1565.58, 1447.48, 1097.09, 754.23; ^{1}H-NMR: δppm: 3.55-3.65 (2H, -CH2-), 4.51 (1H, aniline NH), 11.86 (1H, thiazole NH), 6.54-8.67 (7H, ring CH); MS (m/z): 446.30, 448.10 (M+2) $^+$, 450 (M+4)$^+$

2-((2,4-dichlorophenyl)amino)-N-(4-(2-oxo-2H-chromen-3-yl)thiazol-2-yl)acetamide (13)

Yield: 64%; m.p.: 216-220 ˚C; IR (cm^{-1}): 2923.17, 1714.67, 1604.67, 1482.69, 1253.56, 1095.94, 753.46; ^{1}H-NMR: δppm: 3.54-3.65 (2H, -CH2-), 4.41 (1H, aniline NH), 11.86 (1H, thiazole NH), 6.67-8.67 (7H, ring CH); MS (m/z):446.30 (M)$^+$

2-((2,5-dimethylphenyl)amino)-N-(4-(2-oxo-2H-chromen-3-yl)thiazol-2-yl)acetamide (14)

Yield: 75%; m.p.: 211-215 °C; IR (cm^{-1}): 2921.71, 1715.94, 1605.15, 1555.92, 1096.08, 753.81; ^{1}H-NMR: δppm: 1.20-1.27 & 2.06-2.16 (6H, (-CH3)2), 3.36-3.54 (2H, -CH2-), 4.10 (1H, aniline NH), 11.86 (1H, thiazole NH), 6.87-8.63 (7H, aromatic CH); MS (m/z): 406.25 (M+H) $^{+}$

2-((2,4-dimethylphenyl)amino)-N-(4-(2-oxo-2H-chromen-3-yl)thiazol-2-yl)acetamide (15)

Yield: 69%; m.p.: 188-192 °C; IR (cm^{-1}): 2921.45, 1713.58, 1604.95, 1553.45, 1096.41, 753.54; ^{1}H-NMR: δppm: 1.22-1.29 & 2.09-2.21 (6H, (-CH3)2), 3.34-3.53 (2H, -CH2-), 4.07 (1H, aniline NH), 11.23 (1H, thiazole NH), 6.79-8.64 (7H, aromatic CH); MS (m/z): 406.20 (M+H) $^{+}$

2-((2,3-dimethylphenyl)amino)-N-(4-(2-oxo-2H-chromen-3-yl)thiazol-2-yl)acetamide (16)

Yield: 76%; m.p.: 195-200 °C; IR (cm^{-1}): 2923.71, 1713.73, 1605.15, 1554.46, 1096.22, 754.36; ^{1}H-NMR: δppm: 1.22-1.29 & 2.09-2.21 (6H, (-CH3)2), 3.34-3.53 (2H, -CH2-), 4.07 (1H, aniline NH), 11.23 (1H, thiazole NH), 6.79-8.64 (7H, aromatic CH); MS (m/z): 406.20 (M+H) $^{+}$

2-((2,4-difluorophenyl)amino)-N-(4-(2-oxo-2H-chromen-3-yl)thiazol-2-yl)acetamide (17)

Yield: 84%; m.p.: 217-219 °C; IR (cm^{-1}):2914.10, 1715.20, 1604.98, 1511.48, 1095.80, 754.64; ^{1}H-NMR: δppm: 3.33-3.54 (2H, -CH2-), 4.35 (1H, aniline NH), 11.86 (1H, thiazole NH), 6.77-8.64 (9H, aromatic CH); MS (m/z): 414.10 (M+H) $^{+}$

2-((4-bromophenyl)amino)-N-(4-(2-oxo-2H-chromen-3-yl)thiazol-2-yl)acetamide (18)

Yield: 84%; m.p.: 222-228 °C; IR (cm^{-1}): 2924.10, 1714.72, 1604.61, 1487.69, 1253.67, 755.04; ^{1}H-NMR: δppm: 3.55-3.65 (2H, -CH2-), 4.87 (1H, aniline NH), 12.36 (1H, thiazole NH), 7.11-8.64 (10H, aromatic CH); MS (m/z): 456.31 (M)$^{+}$, MS (m/z): 458 (M+2) $^{+}$

N-(4-(2-oxo-2H-chromen-3-yl)thiazol-2-yl)-2-((3,4,5-trimethoxyphenyl)amino)acetamide (19)

Yield: 76%; m.p.: 229-233 °C; IR (cm^{-1}): 2933.33, 1716.06, 1604.01, 1505.52, 1450.39, 1233.36, 1124.45, 757.06; ^{1}H-NMR: δppm: 3.33-3.71 (9H, (-OCH3)3), 3.73-3.84 (2H, -CH2-), 4.31 (1H, aniline NH), 12.86 (1H, thiazole NH), 7.11-8.64 (8H, aromatic CH); MS (m/z): 467.50 (M)$^{+}$, 468.15 (M+H) $^{+}$

Biological assays

α-glucosidase inhibition assay

The α-Glucosidase enzyme inhibitory activity of the synthesized compound **(5-24)** was determined by mixing 500 µl of 1 mol phosphate buffer $_{PH}$ 6.8, 200 µl of 15 mmol of PNPG (4-Nitrophenyl-β-D-glucopyranoside, SRL) which acted as substrate, 100 µl of 1,2,4,6,8,10 mmol synthesis compound **(5-24)** solution. For this procedure, DMSO was used as solvent. Further, 100 µl of α-Glucosidase enzyme (1/100 Unit, SRL) was mixed with the above mixture and was incubated for 30 min at 37 °C in 1.5 ml of

Eppendorf tubes. 0.15 % of sodium carbonate solution added to end the reaction. Acarbose were used as positive control. Absorbance was measured at 410 nm using a UV spectrophotometer and IC_{50} values were calculated.

References

1. Wondafrash DZ, Desalegn TZ, Yimer EM, et al. Potential Effect of Hydroxychloroquine in Diabetes Mellitus: A Systematic Review on Preclinical and Clinical Trial Studies. J Diabetes Res; 2020. Epub ahead of print 2020. DOI: 10.1155/2020/5214751.

2. Silva SB da, Costa JP, Pintado ME, et al. Antioxidants in the Prevention and Treatment of Diabetic Retinopathy – A Review. J Diabetes Metab; 01. Epub ahead of print 2010. DOI: 10.4172/2155-6156.1000111.

3. Chelladurai GRM, Chinnachamy C. Alpha amylase and alpha glucosidase inhibitory effects of aqueous stem extract of Salacia oblonga and its GC-MS analysis. Brazilian Journal of Pharmaceutical Sciences; 54. Epub ahead of print 2018. DOI: 10.1590/s2175-97902018000117151.

4. Khursheed R, Singh SK, Wadhwa S, et al. Treatment strategies against diabetes: Success so far and challenges ahead. Eur J Pharmacol 2019; 862: 172625.

5. Menteşe E, Baltaş N, Bekircan O. Synthesis and kinetics studies of N'-(2-(3,5-disubstituted-4H-1,2,4-triazol-4-yl)acetyl)-6/7/8-substituted-2-oxo-2H-chromen-3-carbohydrazide derivatives as potent antidiabetic agents. *Arch Pharm (Weinheim)* 2019; 352: 1900227.

6. Hakamata W, Kurihara M, Okuda H, et al. Design and screening strategies for alpha-glucosidase inhibitors based on enzymological information. Curr Top Med Chem 2009; 9: 3–12.

7. Gulçin İ, Taslimi P, Aygün A, et al. Antidiabetic and antiparasitic potentials: Inhibition effects of some natural antioxidant compounds on α-glycosidase, α-amylase and human glutathione S-transferase enzymes. Int J Biol Macromol 2018; 119: 741–746.

8. Yin Z, Zhang W, Feng F, et al. α-Glucosidase inhibitors isolated from medicinal plants. Food Science and Human Wellness 2014; 3: 136–174.

9. Shalini K, Sharma K, Kumar N. Imidazole and its biological activities: A review, .

10. Razzaghi-Asl N, Sepehri S, Ebadi A, et al. Insights into the current status of privileged N-heterocycles as antileishmanial agents. Mol Divers 2020; 24: 525–569.

11. Sari S, Barut B, Özel A, et al. Discovery of potent α-glucosidase inhibitors through structure-based virtual screening of an in-house azole collection. Chem Biol Drug Des 2021; 97: 701–710.

12. Azimi F, Ghasemi JB, Azizian H, et al. Design and synthesis of novel pyrazole-phenyl semicarbazone derivatives as potential α-glucosidase inhibitor: Kinetics and molecular dynamics simulation study. Int J Biol Macromol 2021; 166: 1082–1095.

13. Kumar S, Sharma B, Mehra V, et al. Recent accomplishments on the synthetic/biological facets of pharmacologically active 1H-1,2,3-triazoles. *Eur J Med Chem*; 212. Epub ahead of print 15 February 2021. DOI: 10.1016/J.EJMECH.2020.113069.

14. Singh V, Dogra A, Das J, et al. Brønsted acid functionalized carbon catalyst for synthesis of biologically active coumarin-substituted bis(indolyl)methanes. FlatChem 2021; 29: 100279.

15. M Kretschmer SB, Woltersdorf S, Rödl CB, et al. Development of novel aminothiazole-comprising 5-LO inhibitors. Future Med Chem 2016; 8: 149–164.

16. Saeed A, Ejaz SA, Shehzad M, et al. 3-(5-(Benzylideneamino)thiazol-3-yl)-2 H -chromen-2-ones: a new class of alkaline phosphatase and ecto-5'-nucleotidase inhibitors. RSC Adv 2016; 6: 21026–21036.

17. Mahmood SU, Nazir Y, Saeed A, et al. Synthesis, Biological Evaluation and Molecular Docking Studies of Novel Coumarinylthiazolyl Iminothiazolidinone Hybrids as Potent Urease Inhibitors. ChemistrySelect 2020; 5: 5387–5390.

18. Kanhed AM, Sinha A, Machhi J, et al. Discovery of isoalloxazine derivatives as a new class of potential anti-Alzheimer agents and their synthesis. Bioorg Chem 2015; 61: 7–12.

19. Pistia-Brueggeman G, Hollingsworth RI. A preparation and screening strategy for glycosidase inhibitors. Tetrahedron 2001; 57: 8773–8778.

20. Morris GM, Ruth H, Lindstrom W, et al. AutoDock4 and AutoDockTools4: Automated docking with selective receptor flexibility. J Comput Chem 2009; 30: 2785–2791.

21. Sanner MF. A component-based software environment for visualizing large macromolecular assemblies. Structure 2005; 13: 447–462.

22. Kanhed AM, Dash RC, Parmar N, et al. Benzo[e]pyrimido[5,4-b][1,4]diazepin-6(11H)-one derivatives as Aurora A kinase inhibitors: LQTA-QSAR analysis and detailed systematic validation of the developed model. Mol Divers 2015; 19: 965–974.

23. Huang J, Rauscher S, Nawrocki G, et al. CHARMM36m: an improved force field for folded and intrinsically disordered proteins. Nat Methods 2017; 14: 71–73.

24. Vanommeslaeghe K, Hatcher E, Acharya C, et al. CHARMM general force field: A force field for drug-like molecules compatible with the CHARMM all-atom additive biological force fields. J Comput Chem 2010; 31: 671–690.

25. Yu W, He X, Vanommeslaeghe K, et al. Extension of the CHARMM general force field to sulfonyl-containing compounds and its utility in biomolecular simulations. J Comput Chem 2012; 33: 2451–2468.

26. Mark P, Nilsson L. Structure and Dynamics of the TIP3P, SPC, and SPC/E Water Models at 298 K. Journal of Physical Chemistry A 2001; 105: 9954–9960.

27. Bixon M, Lifson S. Potential functions and conformations in cycloalkanes. Tetrahedron 1967; 23: 769–784.

28. Darden T, York D, Pedersen L. Particle mesh Ewald: An N·log(N) method for Ewald sums in large systems. J Chem Phys 1998; 98: 10089.

Scheme 1

Scheme 1 is available in the Supplementary Files section
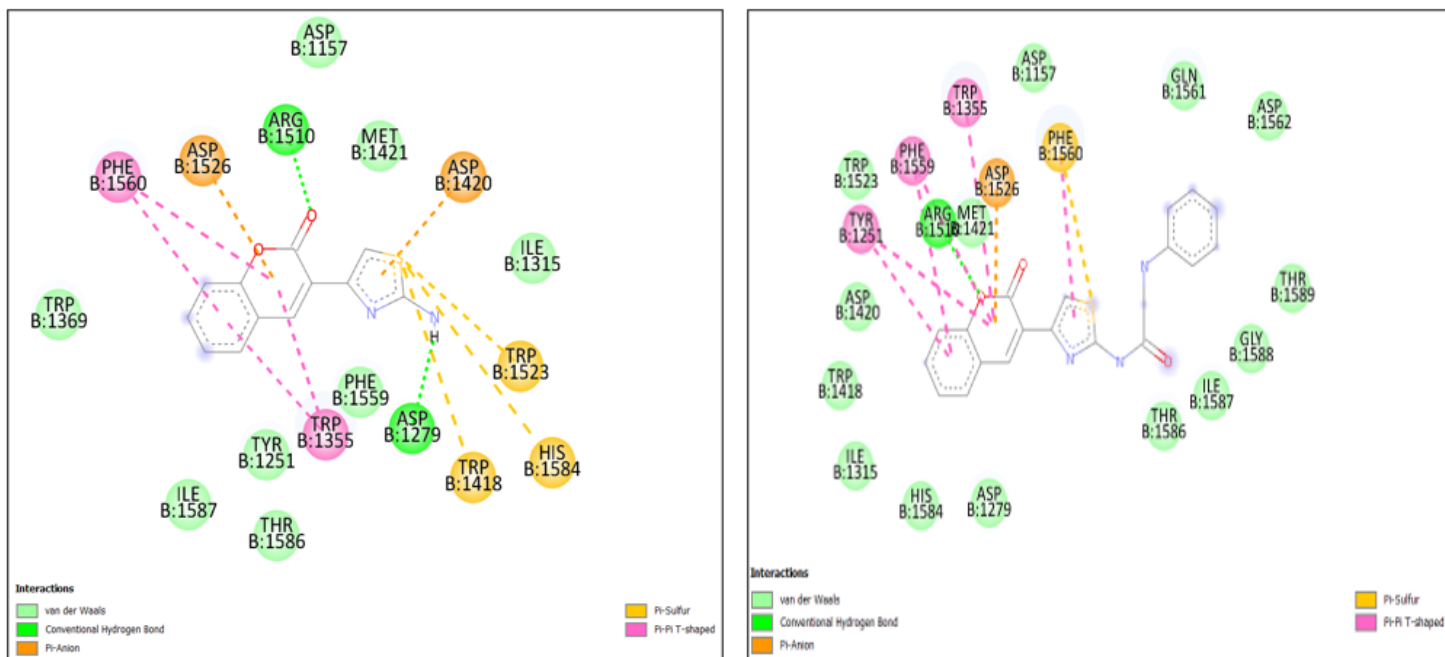
Figures

Figure 1

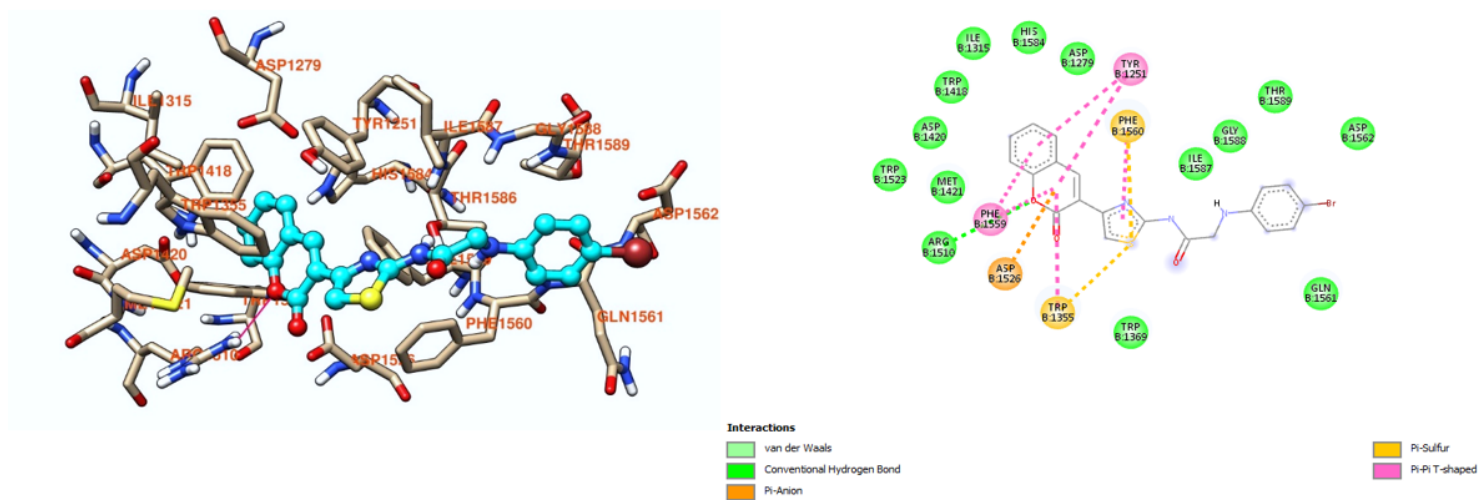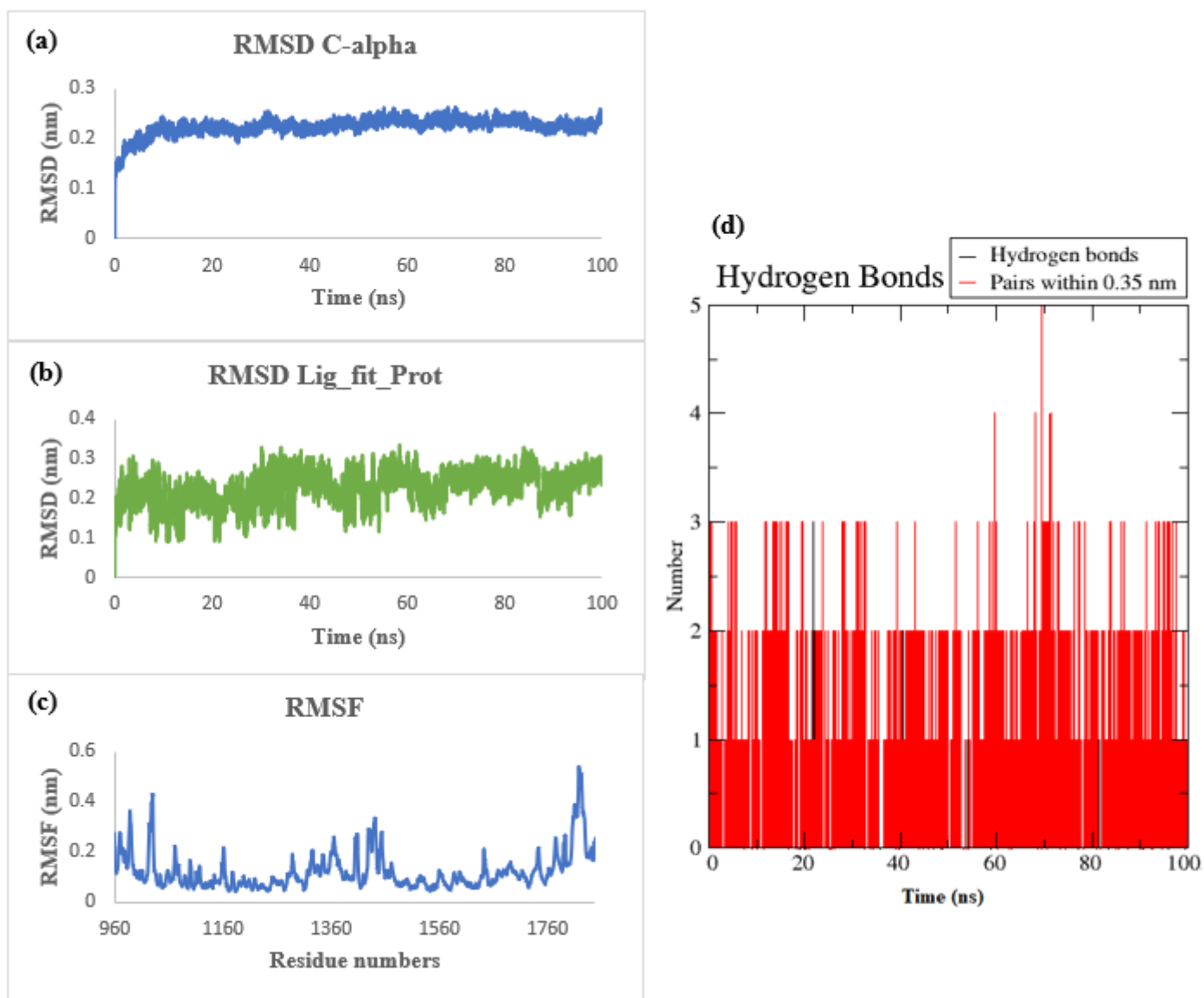Interaction of Scaffold & Aniline with active site pocket with PDB

Figure 2

Molecular docking analysis of most active compound (18) with receptor (PDB code: 3TOP) active site. (a) 3D representation (cyan colour ball and stick model is ligand); (b) 2D representation.

Figure 3

RMSD-P (a), RMSD-L (b), RMSF-P (c), and H-bond plot (d) for α-Glucosidase with compound (18).

Supplementary Files

This is a list of supplementary files associated with this preprint. Click to download.

- Graphicalabstract.jpg
- Scheme1.png
- Supportinginformation.docx